Possibilities and limitations of replacing a conventional corrosion test with an electrochemical potentiokinetic reactivation method using the example of alloy 625

M. Prohaska[a], T. Wernig[a], G. Mori[a], G. Tischler[b], R. Grill[b]

[a]*CD-Laboratory of Localized Corrosion, University of Leoben, Franz-Josef-Straße 18, 8700 Leoben, Austria*
[b]*voestalpine Grobblech GmbH, Voest-Alpine-Straße 3, 4031 Linz, Austria*

Abstract

Susceptibility to intergranular corrosion of nickel-based alloy 625 was investigated by means of a conventional corrosion test (Streicher-test, ASTM G28A) and an electrochemical potentiokinetic reactivation (EPR) test. Stable annealed specimens were sensitized at various times and tested afterwards. The results of both methods were compared and evaluated. Additionally, the influence of various test parameters, e.g. scan rate, vertex potential, solution temperature and activator concentration was investigated. The latter was done for sensitized as well as for non-sensitized specimens. Additional characterization and evaluation was done with a SEM after testing. Advantages and disadvantages of both methods are demonstrated and critically discussed.

Key words: A. alloy 625, B. polarization, C. intergranular corrosion

1. Introduction

The electrochemical potentiokinetic reactivation test (EPR) is a quasi non - destructive test to describe the corrosion resistance of steels and nickel - based alloys. EPR was developed by Cihal et. al. [1] in 1969 with further improvements being made in the following decades. This test is employed primarily to determine the degree of sensitization (DOS), i.e. the materials susceptibility to IGA, but can also provide information on the general corrosion resistance and how this is affected by microstructural changes [2,3]. Compared to conventional corrosion tests, the EPR test exhibits a couple of advantages: It is much quicker, more sensitive and more accurate, particularly for highly sensitizised specimens. In general, two different types of the EPR - test were developed over the years, the double loop [4,5,6] and the single loop [6,7,8] test. In the single loop EPR-test the polarization curve is a reverse curve, with a potential scan from the passive range to open curcuit potential (OCP). In contrast, the double loop EPR-test shows a cyclic polarization curve consisting of a forward scan followed by a reverse scan starting at active OCP. In this case a holding time at a certain vertex potential (usually located in the passive or the transpassive region) is possible. For stainless steels 304 and 304L the EPR-test parameters are prescribed in ASTM G108 [9]. The main focus of this work was the investigation of the susceptibility to intergranular corrosion of the nickel-based alloy 625 after different sensitization times by means of the double loop EPR-test.

Alloy 625 is a wrought nickel - based superalloy strengthened mainly by the addition of carbon, chromium, molybdenum and niobium [10]. Two different types of alloy 625 are available on the market: a low carbon type (less than 0.026% carbon) for wet corrosion applications (normally used in stable annealed condition) and a high carbon type (about 0,045% carbon) for high temperature applications (normally used in solution annealed condition). Typically stable annealing is performed in a temperature range of 940 °C to 980 °C and yields predominantly to primary NbC precipitation and to secondary carbide precipitation of M_6C and NbC. Solution annealing is usually carried out at temperatures

between 1100 and 1150 °C, so solution annealed specimens may contain only primary NbC but no M_6C. Alloy 625 combines the high strength of age-hardened nickel-based alloys with good fabrication characteristics. Furthermore alloy 625 is used as a cladding material for corrosion resistant pipes for oil and gas industry [11]. The fabrication of these pipes is conducted by means of a thermo - mechanical rolling process, which on the one hand improves the mechanical properties of the base material and on the other hand leads to sensitization of the cladding material between 600 – 900 °C. During this sensitization process precipitation hardening takes place in the cladding material. This is mainly due to the precipitation of the metastable η″ -phase $Ni_3(Ni,Al,Ti)$. Furthermore precipitation of $M_{23}C_6$ and M_6C [12,13,14,15] carbides occurs in a temperature range of 660 to 1050 °C, whereas precipitation of MC takes place above 1050 °C. These carbides nucleate preferably on grain boundaries and lead to a depletion of mainly chromium and molybdenum adjacent to the grain boundaries. Hence corrosion resistance in these zones is dramatically reduced and the susceptibility to intergranular corrosion is strongly enhanced. The results described in this paper were determined by means of the EPR-test and the Ferric-Sulfate - Sulfuric-Acid – Test (Streicher-test) according to ASTM G28A. The results of both investigation techniques were compared and evaluated.

2. Experimental method

2.1. Chemical composition and heat treatment parameters of alloy 625

The investigations included in this paper were conducted on sensitized stable annealed clad material. Its chemical composition is shown in tab. 1.

Tab. 1: Chemical composition of alloy 625 acc. to Thyssen Krupp VDM (in weight-%) [16]

material number	Ni	Cr	Mo	Fe	Co	W	Mn	Si	Ti	Nb	C
2.4856	61,09	22,10	9,10	3,50	0,10	0,15	0,04	0,14	0,20	3,42	0,026

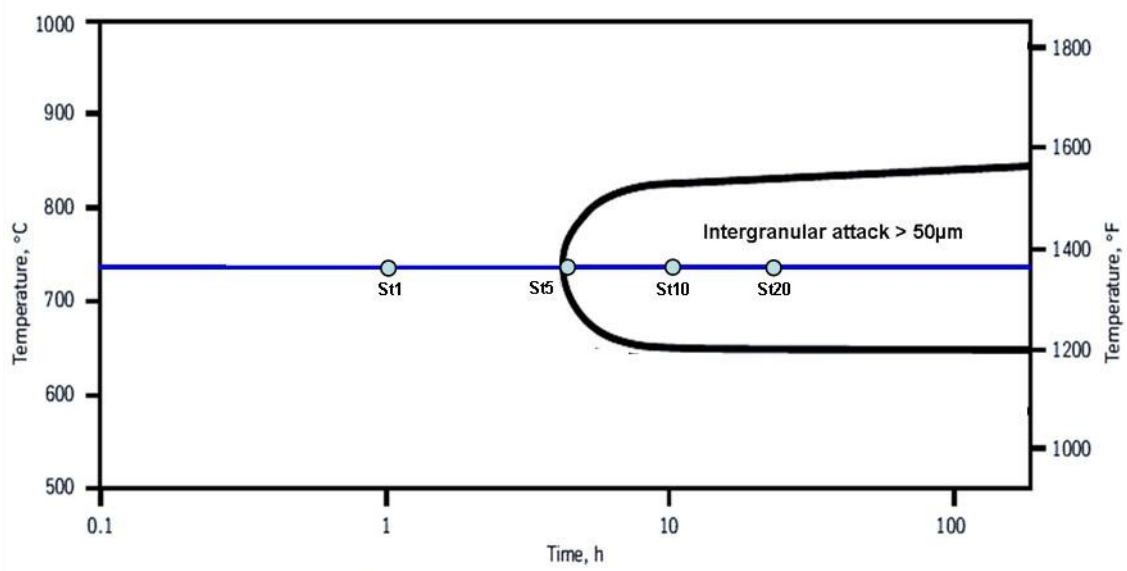

Fig. 1: Heat treatments conducted on stable annealed alloy 625 [16]

The investigated material was manufactured by means of a hot rolling process to a final thickness of 8 mm. Subsequently, stable annealing was done at 960 °C for 3 h. After cutting

to smaller plates additional heat treatments were performed by using electric furnaces under ambient air. The specific heat treatment parameters as well as the sample designation are shown in fig. 1 and tab. 2.

Tab. 2: Heat treatments conducted on stable annealed alloy 625

heat treatment description	sensitization temperature [°C]	sensitization time [h]
St	-	-
St2	740	2
St5	740	5
St10	740	10
St20	740	20

All tested samples were additionally analysed by scanning electron microscopy. The microscope used for the current investigations was a Zeiss Instruments, type "Evo 50".

2.2. Test solution

Streicher-test solution was composed of 236 ml sulfuric acid (H_2SO_4), 25 g iron (III) sulfate hydrate ($Fe_2(SO_4)_3.xH_2O$) and 400 ml distilled water (according G28A). One litre of the used EPR-test solution was composed of 146 ml sulfuric acid (H2SO4), 238 ml hydrochloric acid (HCl) and different amounts of potassiumthiocyanate (KSCN) as an activator (0,0005 to 0,01 mol/l) mixed with laboratory-grade distilled water.

2.3. Test procedure

First of all, it was necessary to determine a suitable EPR-test procedure (that means selection of test parameters and solution composition). To enable evaluation of intergranular and uniform attack by means of light and scanning electron microscopy, all samples (for Streichertest as well as for EPR-test) were surface-finished using final 1200-grit abrasive SiC-paper followed by polishing with 3 microns diamond suspension. The test procedure of the EPR-test was according to ASTM G108, with some modifications: All samples had to be in an active condition when immersed into the test solution. Therefore, the measurement had to be started within a maximum delay of 3 minutes after polishing and cleaning with acetone. Reason for that small time frame was the avoidance of a formation of an overly thick protective oxide layer. After pouring the solution into the electrochemical cell, a delay of 40 min was maintained to assure homogenous temperature of the test solution. Argon was used to stir the solution during the experiment to ensure an oxygen-free electrolyte. The open circuit potential (OCP) was measured for 2 min and there was no delay at the vertex potential. The current density ratio (Ir/Ia) was calculated and evaluated. The Streicher-test was performed at a temperature of boiling sulfuric acid for a time of 120 h. The test procedure was carried out strictly according to ASTM G28A.

The effect of the performed heat treatments on susceptibility to intergranular corrosion was investigated by means of EPR- and Streicher-tests.

Optical microscopy (type Zeiss "Axio Imager") was used to evaluate the most suitable test parameters by examining the extent of uniform corrosive attack in comparison to the extent of intergranular corrosive attack.

The chosen parameters for the EPR-test to detect susceptibility to intergranular corrosion of stable annealed alloy 625 is obvious in tab. 5.

3. Results

3.1. Evaluation of optimized EPR-test parameters

All investigations concerning optimized test parameters were carried out on sensitized and non-sensitized specimens (nomenclature “St”and “St20”). The influence of scan rate, vertex potential, solution temperature and activator concentration on the EPR-test results was examined (tab. 3). Optical microscopy was used to determine the microstructure of the samples.

Tab. 3: Overview of investigated EPR-test parameters for stable annealed alloy 625

scan rate [mV/ s]	vertex potential [mV]	solution temperature [°C]	activator concentration [mol/l]
0,56	200	30	0,001
1,12	200	30	0,001
1,67	200	30	0,001
2,23	200	30	0,001
5,05	200	30	0,001
1,67	75	30	0,001
1,67	180	30	0,001
1,67	220	30	0,001
1,67	300	30	0,001
1,67	200	28	0,001
1,67	200	32	0,001
1,67	200	30	0,0005
1,67	200	30	0,002
1,67	200	30	0,01

3.1.1. Scan rate

The Ir/Ia ratio decreased considerably with increasing the scan rate (fig. 2a and 2b). This tendency was also determined in case of a different activator (H_2NCSNH_2) by Huang. et. al [17].

3.1.2. Vertex potential

The current density ratio (Ir/Ia) decreases considerably with increasing the vertex potential. This correlation is shown in fig. 2c and 2d.

3.1.3. Solution temperature

The dependency of Ir/Ia ratio on temperature is shown in fig. 2e and 2f. The higher the solution temperature, the higher the current density ratio.

3.1.4. Activator concentration

The current density ratio first rises heavily with increasing concentration of KSCN but at higher concentrations, the slope of the curve decreases considerably (fig. 2g and 2h).

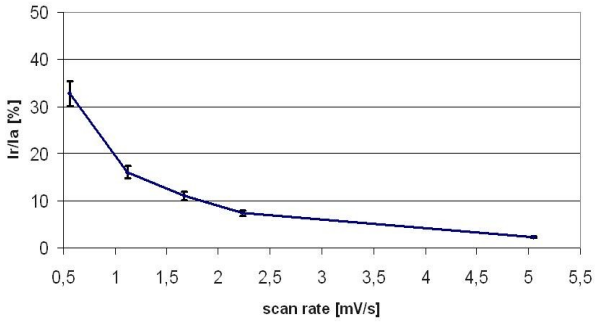

a) Influence of scan rate on the current density ratio (St)

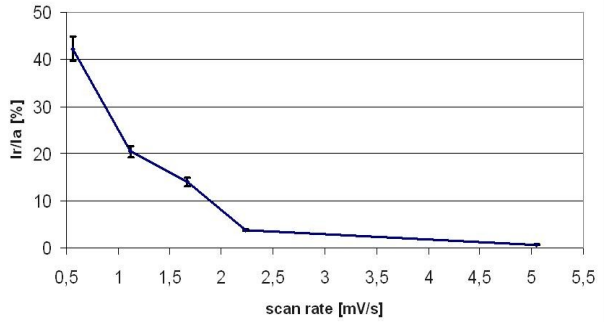

b) Influence of scan rate on the current density ratio (St20)

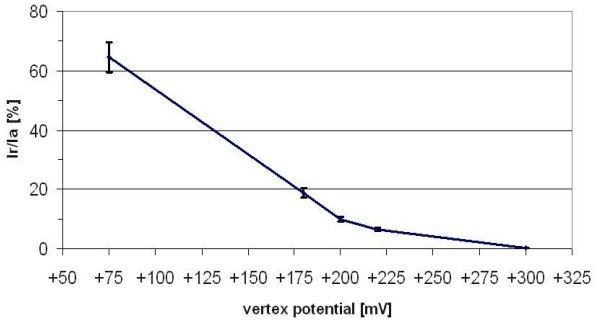

c) Influence of vertex potential on the current density ratio (St)

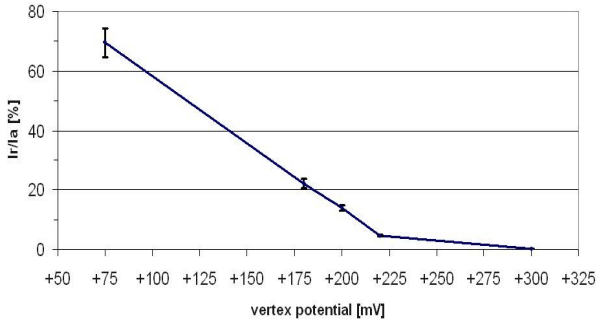

d) Influence of vertex potential on the current density ratio (St20)

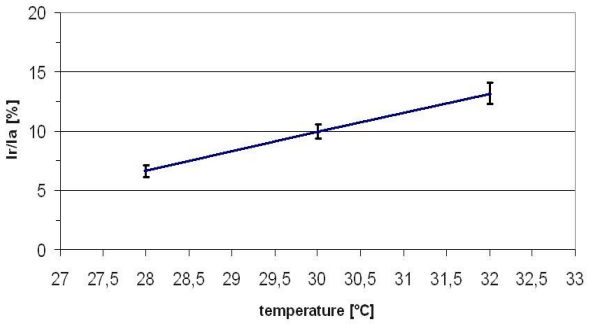

e) Influence of solution temperature on the current density ratio (St)

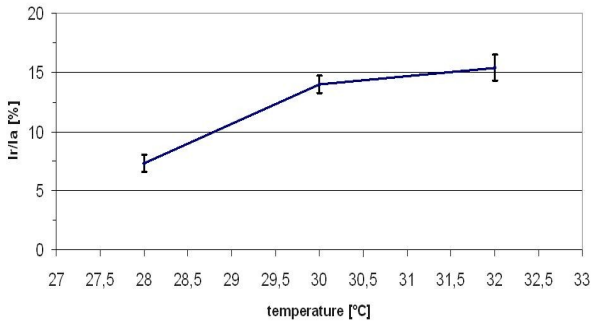

f) Influence of solution temperature on the current density ratio (St20)

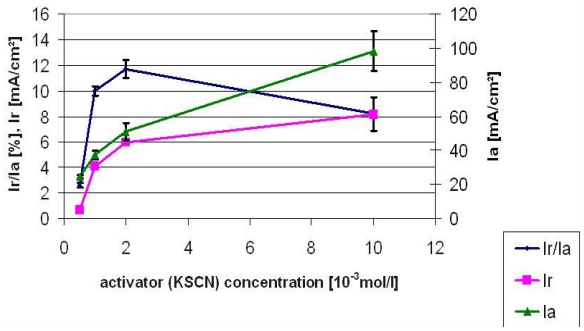

g) Influence of activator concentration on the current density (ratio) (St)

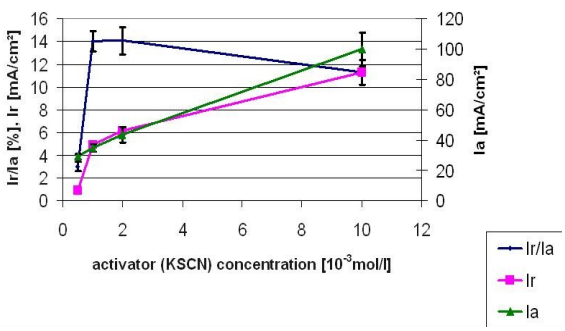

h) Influence of activator concentration on the current density (ratio) (St20)

Fig. 2: Influence of certain parameters on the EPR-test results

3.2. Comparison of Streicher-test and EPR-test

Fig. 3 and fig. 4 show the results of Streicher-test and those of EPR-test.

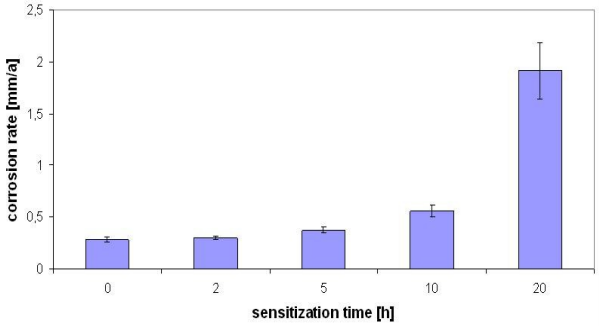

Fig. 3: Corrosion rate of Streicher-tests as function of sensitization time

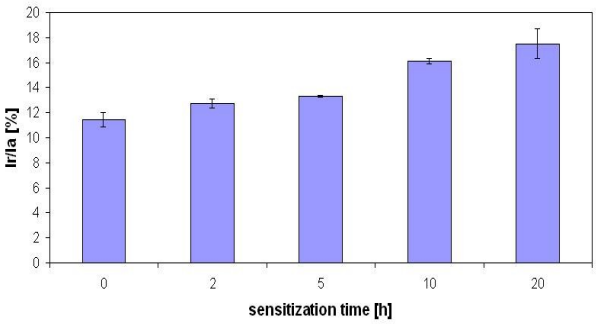

Fig. 4: Ir/Ia values of EPR-tests as function of sensitization time

The corrosion rate of investigated samples only slightly increased during the Streicher-test up to a time of 10 h after which time a sharp increase between 10 an 20 hours of sensitization was observed (fig. 3). Additionally, the standard deviation of the performed Streicher-tests continuously increased with longer sensitization times, too. The Ir/Ia-ratios determined in the EPR-test initially showed similar dependency as the Streicher-tests, but the large increase was not seen after 10 hours of sensitization, indeed there appeared to be almost no further increase in the Ir/Ia-ratios after 20 hours of sensitization (fig. 4).

3.3. 3-dimensional Light Microscopy Characterization

In order to quantificate the extent of dissolved material during Streicher-tests, investigations by means of a 3-dimensional light microscope (type “alicona imaging Infinite Focus G3”) were performed. Analysis was done by using the “area analysis”-function of software “IFM 2.2”. Relevant surface parameters (V_{vv} and S_{vk}) for sample characterisation were evaluated for most sensitized as well as for non- sensitized specimens. V_{vv} is contributed to the amount of dropped grains, whereas the parameter S_{vk} discribes the average depth of surface voids caused by grain dropping. A detailed explanation of the evaluated surface and volume parameters is presented in fig. 5. Fig. 6 shows measured bearing load curves of sensitized and non-sensitized alloy 625. It is obvious that the valley void volume as well as the reduced valley height (nomenclature according fig. 5) is higher after 20 h of sensitization.

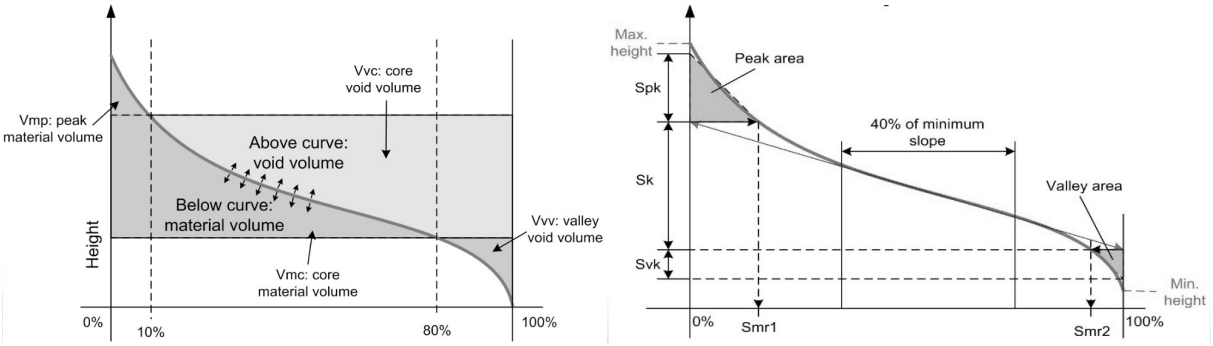

Fig. 5: Volume and surface parameters according «alicona imaging» software «IFM2.2»[18]

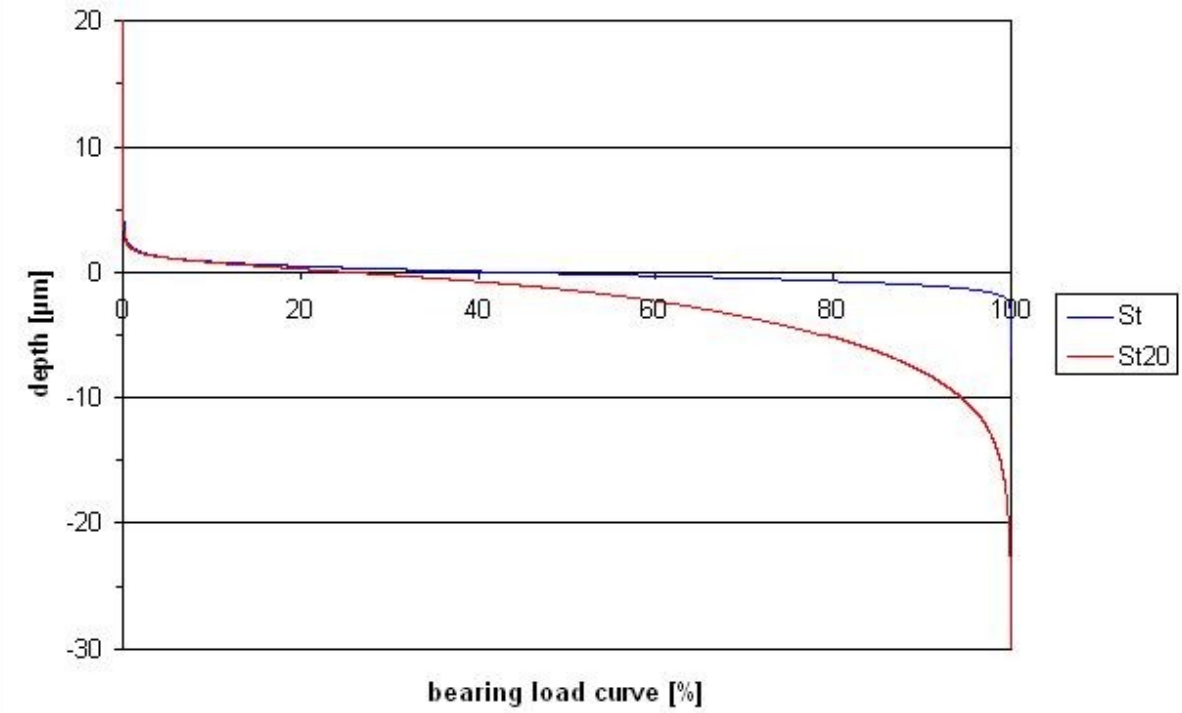

Fig. 6: Bearing load curve of non-sensitized and sensitized stable annealed alloy 625

The quantitative results of 3-dimensional light microscopy are shown in tab. 4. Each heat treatment condition was measured three times.

Tab. 4: Sample surface characterisation after Streicher-tests

heat treatment description	sensitization temperature [°C]	sensitization time [h]	valley void volume (V_{vv}) [ml/m²]	reduced valley height (S_{vk}) [µm]
St	-	-	0,09 ± 0,004	0,86 ± 0,04
St10	740	10	0,25 ± 0,01	2,53 ± 0,02
St20	740	20	0,75 ± 0,02	7,74 ± 0,11

Depth of attack as well as dissolved volume increases slightly until a sensitization time of 10 h. After sensitization for 20 h the values of both surface parameters have noticeable high values. These results are completely consistent with corrosion rate evaluated by means of Streicher-test (fig. 3).

3.4. Scanning Electron Microscopy (SEM) Characterization

Fig. 7 illustrates SEM-images of stable annealed specimens investigated in the Streicher-test. The longer the sensitization time the higher is the corrosive attack (fig. 7a, 7c and 7e). A considerable amount of grains dropped after 20 h of sensitization. As determined by means of Streicher-test and 3-dimensional microscopy, susceptibility to intergranular corrosion increased with longer sensitization times.

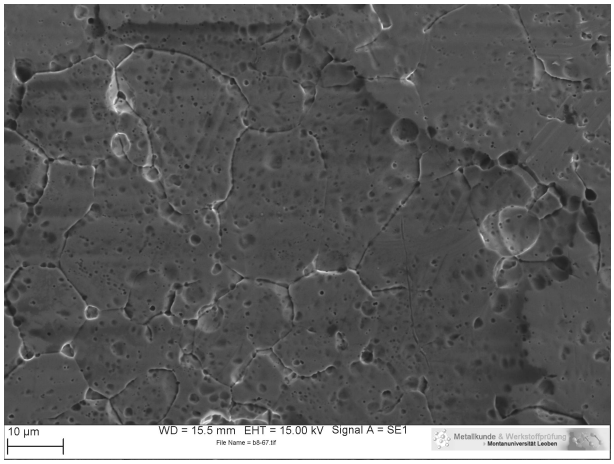

a) Microstructure after Streicher-test (St)

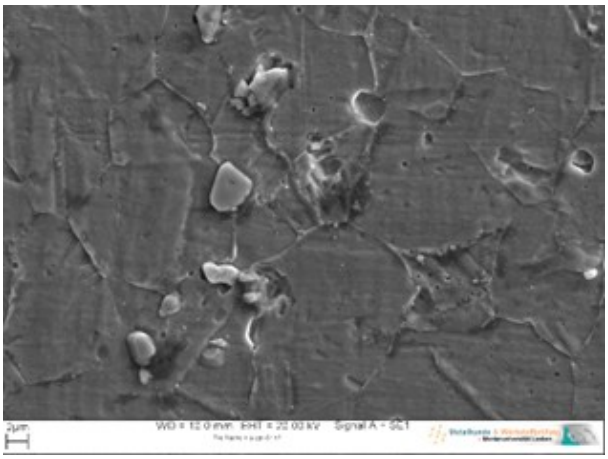

b) Microstructure after EPR-test (St)

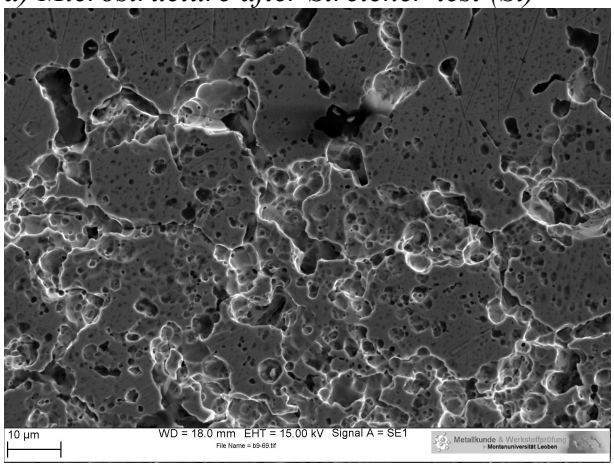

c) Microstructure after Streicher-test (St10)

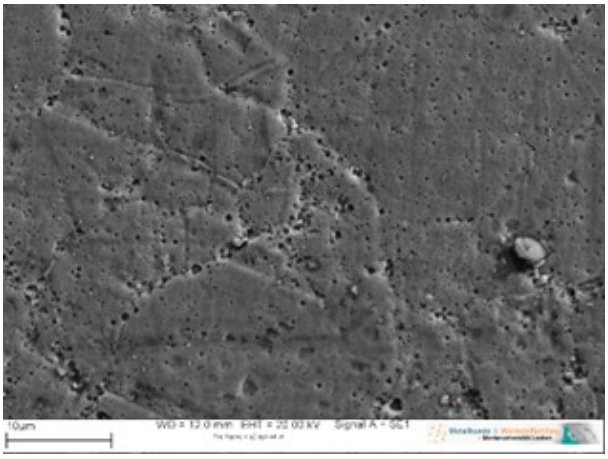

d) Microstructure after EPR-test (St10)

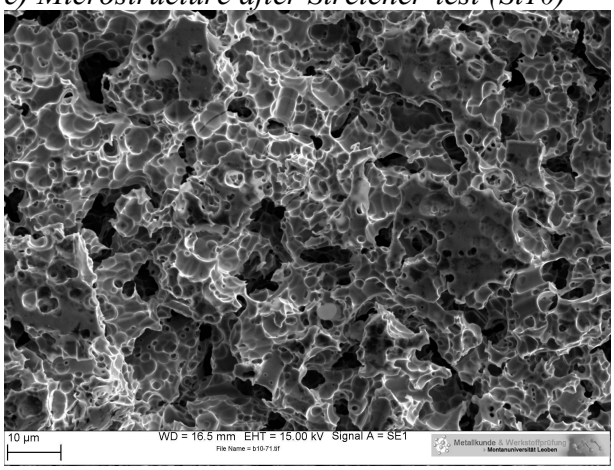

e) Microstructure after Streicher-test (St20)

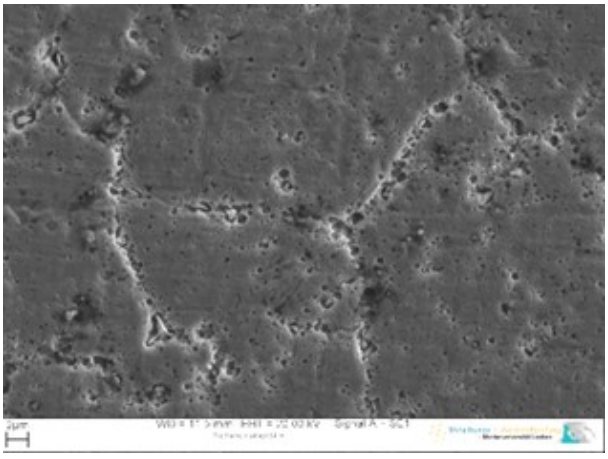

f) Microstructure after EPR-test (St20)

Fig. 7: Microstructural characterisation of Streicher- and EPR-tests by means of SEM

This dependency was also examined by using the EPR-method. Fig. 7b, 7d and 7f show images of stable annealed samples after various sensitization times. It is obvious, that intergranular attack occurred increasingly with time of sensitization. The morphology of the corrosive attack was increasingly localized at grain boundaries.

4. Discussion

4.1. EPR-test parameters

4.1.1. Scan rate

If the scan rate is high, there is less time for dissolution of the metal at the grain boundaries and only marginal uniform attack and a negligible extent of intergranular corrosion takes place. This is accompanied by a very low Ir/Ia ratio. If the scan rate is low, the passive layer formed in the passive region of the specimen during the EPR-test is destroyed and metal dissolution emerges preferably around the grain boundaries in the chromium and molybdenum depleted zones, but also intragranularly. Thus, the determined current density during reactivation (Ir) is very high because of a considerable extent of uniform corrosion. This results in a high Ir/Ia ratio. The Ir/Ia ratio is, as expected, constantly higher for sensitized specimens compared to non-sensitized specimens, but the dependency of the vertex potential is the same for all tested specimens.

4.1.2. Vertex potential

The higher the vertex potential, the more protective is the passive layer on the specimen surface and therefore, metal dissolution in the reverse scan is impeded. If the vertex potential is too high (e.g. 300 mV - fig. 2c and 2d), no metal dissolution, not even at the grain boundaries, during reactivation occurs and the current density ratio is almost zero. Otherwise, if the vertex potential is too low, the passive layer in the non-sensitized zone cannot form either and uniform corrosion takes place. Fig. 8 shows micrographs of stable annealed, non-sensitized specimens after EPR-testing with a vertex potential of 180 mV and 220 mV, respectively. A small increase of the vertex potential from +180 mV (fig. 8a) to +220 mV (fig. 8b) lowers the extent of uniform corrosion considerably.

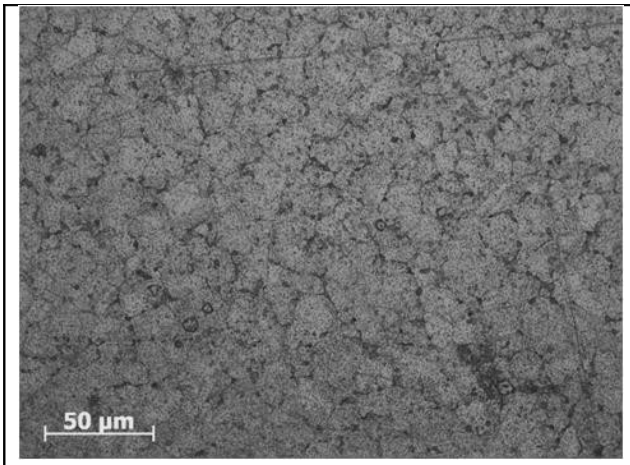

a) vertex potential: 180 mV (St)

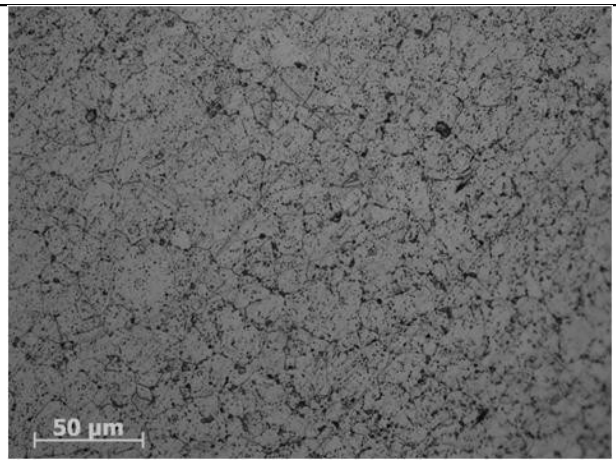

b) vertex potential: 220 mV (St)

Fig. 8: Microstructural characterisation of EPR-samples after testing with different vertex potentials, non-sensitized condition

4.1.3. Solution temperature
The current density ratio increases with increasing the solution temperature due to a higher metal dissolution rate at high temperatures in aggressive media. Thus, solution temperature has to be controlled very accurately.

4.1.4. Activator concentration
A high amount of KSCN in the solution enhances the metal dissolution during activation as well as during reactivation (fig. 2g and 2h). The increase of the activation current was almost constant with increasing activator concentration. Contrarily, the increase of the reactivation current declined with increasing concentration of the activator. Therefore the ratio Ir/Ia peaks near 0,002 mol/l. If the activator concentration is too high, e.g. 0,01 M, uniform corrosion occurs on the surface of the specimen to a very high extent. The activator concentration used in this series of experiments (0,001 mol/l) is a good compromise between high resolution and sensitivity of the EPR-test, on the one hand and avoidance of uniform corrosion, on the other hand.

The influences of scan rate, vertex potential, solution temperature and activator concentration on the current density ratio show no significant dependency on previous heat treatments of the specimens. Therefore, the influence of test parameters on the results is considerably stronger than the resolution of the EPR-test itself. So the parameters have to be chosen very carefully before beginning a new measurement series. Additionally, it is recommended to check the solution temperature always before starting the EPR-measurements to achieve comparable as well as reliable results.

Finally it was examined that the following EPR-test parameters showed the most promising results (tab. 5):

Tab. 5: Suitable parameters for the EPR-test

scan rate [mV/s]	vertex potential [mV]	solution temperature [°C]	activator concentration [mol/l]
1,67	200	30	0,001

4.2. Comparison of Streicher- and EPR-test

During Streicher-test amount of corrosive attack is determined by quantity of dissolved volume of chromium/molybdenum depleted zones as well as by the amount of dropped grains. The higher the sensitization of the specimen the higher the amount of dropped grains and therefore, the influence of dissolved volume on the calculated corrosion rate decreases. When continuous dissolution of grain boundaries occurs, corrosion rate during Streicher-test peaks because grain dropping is promoted.
Besides, EPR-test is sensitive to the sensitized volume at, or connected to, the specimen's surface. Therefore, a deep and wide corrosive attack leads to a high EPR-value. Continuity of the corrosive attack is not as strinking as for the Streicher-test to reach high values.

The corrosion rate evaluated via Streicher-test was rather small, but after 10 h of isothermal heat treatment at 740 °C it rose sharply. It was found that apart from the moderately increasing susceptibility to intergranular corrosion the amount of dropped grains had strongly enlarged.

The Ir/Ia ratio determined by means of EPR-test increased only slightly but almost constantly with increasing sensitization time. In the stable annealed condition, alloy 625 exhibits a considerable amount of primary NbC, (Nb,Ti)C and especially M_6C. Therefore, Ir/Ia values are rather high even without additional sensitization treatment. Primary NbC causes a reduction of the effective carbon content in the matrix. Thus, further carbide precipitation during sensitization is impeded and the increase of Ir/Ia-values with increasing sensitization times is low.

5. Conclusions

In the present work sensitization of alloy 625 has been investigated with Streicher-tests (ASTM G28A) and EPR-tests. Additionally, the influence of certain test parameters on the results of EPR-test has been examined.
EPR-test is highly dependent on size of chromium and molybdenum depleted zones. Corrosion rate calculated on the basis of mass loss during Streicher-test is only partially caused by size of chromium and molybdenum depleted zones, but also by the amount of dropped grains. In case of experiments prescribed in this paper, both corrosion tests show comparable results, although the EPR-test is more sensitive at low degrees of sensitization (DOS), when only a negligible extent of grain dropping occurs.

It is possible to replace the Streicher-test by the EPR-test, with some restrictions: First of all, it has to be assured, that the whole EPR-test procedure is carried out very accurately and precisely. The influence of the test procedure (especially avoidance of the formation of an overly thick passive film and selection of test parameters) is much stronger compared to the Streicher-test. Test parameters have to be selected in a way, that only a minor extent of uniform corrosion occurs during the test. Additionally it has to be considered, that mass loss evaluated by means of Streicher-test is strongly influenced by amount of dropped grains, whereas during EPR-test no grain dropping occurs. The current density ratio is directly related to the extent of dissolved specimen volume and thus, to the degree of sensitization.

In summary, the EPR-technique is a promising investigation technique for detecting susceptibility to intergranular corrosion in nickel-based alloys, especially for research in laboratories (short testing time). However, it has to be considered that specimen characterisation by means of light and/or scanning electron microscopy is absolutely necessary after EPR-tests to confirm the measured current density ratios and to determine the type of attack. If applying the EPR-method in the field, the sensitive test procedure might be a problem, especially when investigations on highly alloyed materials, e.g. nickel-based alloys, have to be executed.

References

[1] V. Číhal, T. Shoji, V. Kain, Y. Watanabe, R. Stefec, “Electrochemical Polarization Reactivation Technique: EPR-a Comprehensive Review”, in: Fracture and Reliability Research Institute, Graduate School of Engineering, Tohoku University, 2004.

[2] U. Mudali, R. Dayal, J. Gnanamoorthy, P. Rodriguez, “Relationship between Pitting and Intergranular Corrosion of Nitrogen-bearing Austenitic Stainless Steels”, in: ISIJ International 36 (7) (1996) 799–806.

[3] A. Turnbull, P. Francis, M. Ryan, L. Orkney, A. Griffiths, B. Hawkins, “A novel approach to characterizing the corrosion resistance of super duplex stainless steel welds”, in: Corrosion (Houston, Tex.) 58 (12) (2002) 1039–1048.

[4] R. Kilian, „EPR Round Robin Test mit sensibilisierten austenitischen Stählen Teil 1: Auswertung der Ergebnisse nach dem JIS-Verfahren“, in: Materials and Corrosion 52 (2001) 45–53.

[5] S. Schultze, J. Goellner, J. Panitz, „EPR-Messungen in warmgehenden Anlagen“, in: Materials and Corrosion 54 (12) (2003) 958–965.

[6] P. Záhumensky, S. Tuleja, J. Országová, J. Janovec, V. Siládiová, “Corrosion resistance of 18Cr-12Ni-2, 5Mo steel-annealed at 500–1050 ◯C”, in: Corrosion Science 41 (7) (1999) 1305–1322.

[7] V. Čıhal, R. Štefec, “On the development of the electrochemical potentiokinetic method”, in: Electrochimica Acta 46 (24-25) (2001) 3867–3877.

[8] S. Kumar, M. Banerjee, “Improvement of Intergranular Corrosion Resistance of Type 316 Stainless Steel by Laser Surface Melting”, in: Surface Engineering 17 (6) (2001) 483–489.

[9] Annual Book of ASTM Standards; Section 3: Metals Test Methods and Analytical Procedures; Volume 03.02: Wear and Erosion, Metal Corrosion, ASTM, 2000.

[10] U. Heubner, „Nickel Alloys“, in: CRC Press, 1998.

[11] R. Schimboek, G. Heigl, R. Grill, T. Reichel, J. Beissel, U. Wende, “Clad pipes for the oil and gas industry–manufacturing and applications”, in: Proceedings of Stainless Steel World United Pipelines (2004) 375–393.

[12] M. Sundararaman, P. Mukhopadhyay, S. Banerjee, “Carbide precipitation in nickel base superalloys 718 and 625 and their effect on mechanical properties”, in: Superalloys 718 625–706.

[13] L. Ferrer, B. Pieraggi, J. Uginet, “Microstructural Evolution During Thermomechanical Processing of Alloy 625”, in: Superalloys 718, 625, 706 and various derivatives, TMS, (1991), 217-228

[14] M. Köhler, U. Heubner, “The effect of final heat treatment and chemical composition on sensitization, strength and thermal stability of alloy 625”, in: Superalloys 718,625, 706 and Various Derivatives; The Minerals, Metals & Materials Society (1997) 795–803.

[15] V. Shankar, K. Bhanu Sankara Rao, S. Mannan, “Microstructure and mechanical properties of Inconel 625 superalloy”, in: Journal of Nuclear Materials 288 (2-3) (2001) 222–232.

[16] Material Data Sheet No. 4018: „Corrosion-resistant and high-temperature Alloy Nicrofer 6020 hMo – Alloy 625“, (2007), Thyssen Krupp VDM

[17] H. Huang, C. Liu, S. Chen, “Electrolyte System of EPR Test for Detecting Sensitization in Austenitic Stainless Steel”, in: Corrosion, 48 (1992) 509–513

[18] Alicona Imaging GmbH - Area Analysis Automation Manual, IFM 2.2, Infinite Focus G3